Available online at www.sciencedirect.com

SCIENCE DIRECT®

Lithos 83 (2005) 183–198

LITHOS

www.elsevier.com/locate/lithos

A mantle or mafic crustal source for Proterozoic anorthosites?

John Longhi*

Lamont-Doherty Earth Observatory, Palisades, NY 10964, USA

Received 25 February 2004; accepted 18 February 2005
Available online 22 April 2005

Abstract

Calculations of fractional crystallization (FC) and assimilation fractional crystallization (AFC) at 11 kb for a variety of primitive magmatic compositions and a mafic assimilant demonstrate that none of them has a bulk composition suitable to be parental to massif anorthosites. Mafic compositions thought to be parental to massif anorthosites have Mg′ values of 0.6 to 0.4 and form coherent arrays with moderately steep slopes on plots of TiO_2, K_2O, and P_2O_5 versus Mg′. The calculated liquid lines of descent (LLD) of basaltic magmas undergoing FC or AFC processes pass through the arrays of anorthosite parent magma compositions with much shallower slopes than the natural arrays, which indicates that the arrays of natural parental magmas were produced by a process other than FC/AFC. Also, by the time most crystallizing basaltic magmas with or without assimilation reach plagioclase saturation, their residual liquids have Mg′ values that are too low to be parental to anorthosites. MORB-like olivine tholeiites and high-aluminum olivine tholeiites (HAOT) from convergent plate margins do reach plagioclase saturation while sufficiently magnesian, but their Wo (Wollastonite) contents are too high such that they reach plagioclase saturation coexisting only with augite and do not reach orthopyroxene saturation (if at all) until Mg′ is too low. Calculations show it is not possible to produce a high-Al melt from typical mantle peridotites that has sufficient TiO_2 to make andesine-type anorthosite.

Calculation of partial melting for an average mafic crustal composition at 11 kbar provides a much closer match to the array of natural parental compositions in terms of minor element concentrations and proportions of mineral components. However, accounting for the entire array requires a more magnesian source composition. Such compositions exist in several crustal xenolith localities. Similar results were obtained using the bulk composition of the Stillwater Complex, which is used as a model mafic source (here the premise is that overdense crustal intrusions might sink back into the mantle). As with the terrain composition, this particular layered intrusion composition is not sufficiently magnesian, however, the fit improves when mixtures of early and late stage portions of the complex (i.e., the denser portions) were run as potential source regions.

Keywords: Partial melting; Proterozoic anorthosite; Assimilation; Fractional crystallization; Mafic crust

1. Introduction

A majority of workers believe that Proterozoic (massif) anorthosites formed in two stages. The first stage entails formation of plagioclase-rich suspen-

* Tel.: +1 845 365 8659; fax: +1 845 365 8155.
E-mail address: longhi@ldeo.columbia.edu.

0024-4937/$ - see front matter © 2005 Elsevier B.V. All rights reserved.
doi:10.1016/j.lithos.2005.03.009

sions in deep-seated chambers, followed by intrusion of the suspensions into mid to upper crustal chambers that, together with associated mafic and granitic intrusions, comprise the igneous complexes we observe today. Mineral assemblages in the contact metamorphic aureoles of the massif intrusions record pressures in the range of 3–6 kbar (Berg, 1977; Jansen et al., 1985), thus locating emplacement of the massifs in the middle to upper crust. The preponderance of lithologies with plagioclase well in excess of cotectic proportions (Duchesne, 1984; Emslie, 1985) forms the basis for positing that the massifs were formed from suspensions of plagioclase in basaltic liquid, intruded from below. Nearly ubiquitous highly aluminous orthopyroxene megacrysts (HAOM), whose compositions record maximum pressures in the range of 10–13 kbar (Longhi et al., 1993; Maquil and Duchesne, 1984) and which are commonly intergrown with plagioclase megacrysts, provide the evidence for lower crustal/upper mantle magma chambers in which the plagioclase-rich suspensions developed. A major point of contention is whether these deep-seated chambers represent ponded magma derived from melting typical peridotitic mantle (Emslie et al., 1994), or in situ melt of mafic sources (Duchesne, 1989; Longhi et al., 1999), or partial melting of anomalous, Fe- and Al-enriched mantle (Olsen and Morse, 1990). Isotope analyses show definite contributions of crustal components (Ashwal and Wooden, 1983; Emslie et al., 1994; Scoates and Frost, 1996). The proportion of the crustal component distinguishes the first hypothesis from the latter two. Separating the latter two may not be straightforward.

2. Calculations

In order to test the conflicting hypotheses, a series of calculations were performed simulating fractional crystallization, fractional crystallization with assimilation, and partial melting. The calculations were carried out with versions of the MAGFOX and MAGPOX (BATCH) programs developed by the author (Longhi, 1991; Longhi, 2002) and presently modified to accommodate high-pressure fractional crystallization and to conform to the experimental phase equilibria reported by Longhi et al. (1999). Copies of the application or source codes are available from the author.

Although the natural processes surely take place over a range of pressures, most of the calculations were carried out for a single pressure to conform with the most common representation of the first stage of anorthosite petrogenesis, namely, that of a ponded magma body interacting with the lower crust (e.g., Ashwal, 1993). The pressure of 11 kbar was chosen to accommodate (a) the high pressure record of the HAOM (Longhi et al., 1993; Maquil and Duchesne, 1984) and (b) the observations that two very different proposed parental magmas, HLCA (Emslie, 1980) and TJ (Duchesne and Hertogen, 1988), are multiply saturated with plagioclase and pyroxene in the range of 11–13 kbar (Fram and Longhi, 1992; Vander Auwera and Longhi, 1994). A set of polybaric fractional fusion calculations, modified after Longhi (1992 and 2002), was also carried out to shed some light on the direct mantle-melting hypothesis.

3. Results and discussion

Fig. 1 illustrates four groups of igneous compositions and the traces of four fractional crystallization paths at 11 kbar. The four groups include a representative subset of primitive basaltic compositions (triangles) compiled by BVSP (1981), a compilation from Longhi et al. (1999) of mafic magmatic compositions (squares) proposed by various authors to be parental or at least related to massif anorthosites, mafic rock compositions from the Harp Lake complex reported by Emslie (1980), and a set of granitoids associated with massif anorthosites in Nain, Labrador (Emslie, 1991) and Rogaland, Norway (Duchesne and Wilmart, 1997). The primitive basalt compositions have the highest Mg′ (Mg′=MgO/[MgO+FeO] molar) values of the plotted compositions and thus are plausible starting points for the general proposition that Proterozoic anorthosites are derived by interaction of basaltic magma with continental crust.

The set of incompatible minor elements that are plotted (Ti, K, P) in Fig. 1 is typically more abundant in mafic rocks associated with massif anorthosites than in most basaltic suites. Also, they exhibit different geochemical properties: Ti and P are high field strength elements that are far more soluble in

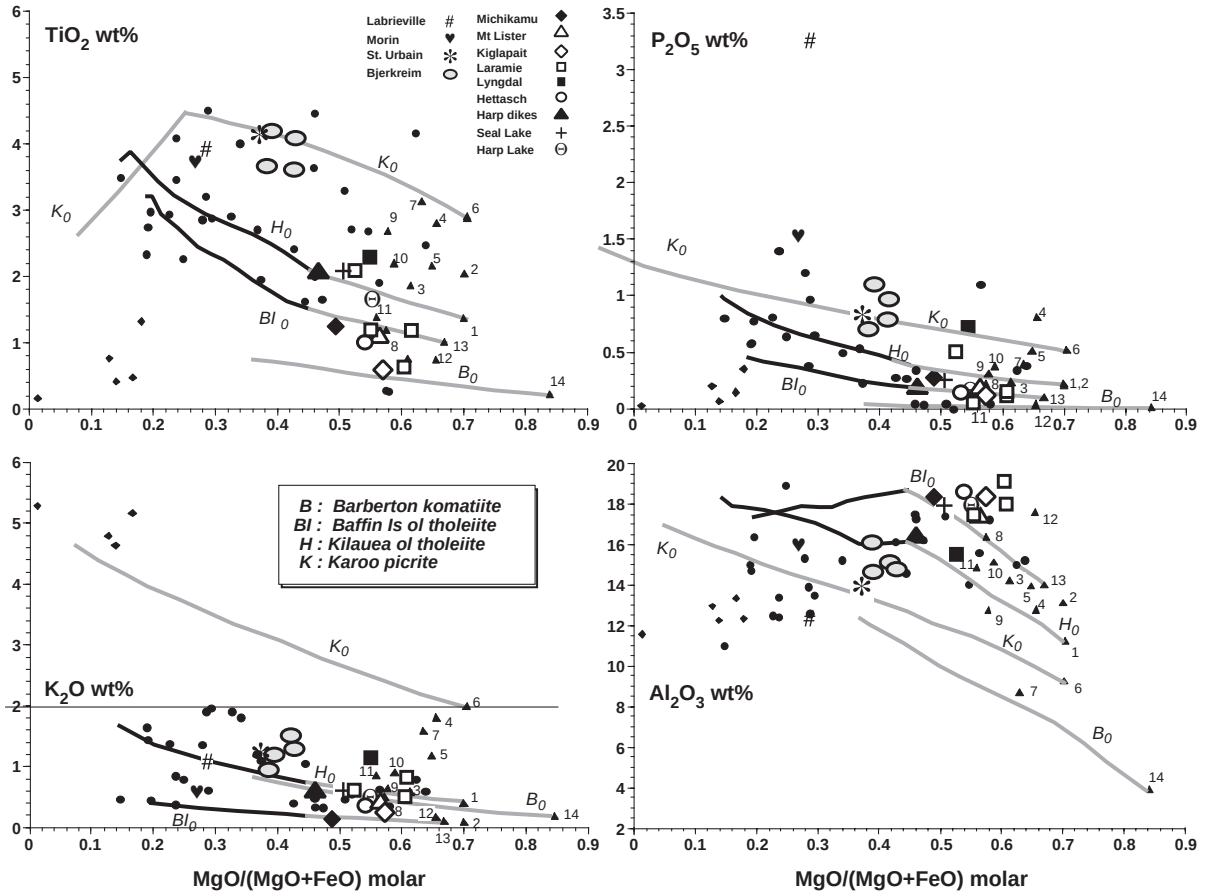

Fig. 1. Calculated fractional crystallization (no assimilation) paths of primitive basaltic magmas. Curves are fractional crystallization (80%) paths calculated with a version of MAGFOX (Longhi, 1991) modified for high pressure (here 11 kb). Solid portions of the curves correspond to plagioclase saturation. Starting compositions (H=Hawaii; BI=Baffin Island; K=Karoo; B=Barberton komatiite) listed in Table 1. Large symbols are a suite of proposed anorthosite parent magmas (Longhi et al., 1999); small filled circles=mafic rock compositions from the Harp Lake Anorthosite Complex (Emslie, 1980); diamonds=granitoids (Duchesne and Wilmart, 1997; Emslie et al., 1994); numbered triangles=primitive basaltic magmas from BVSP (1981)—1,2=Hawaiian olivine tholeiites (Table 1.2.6.14); 3=alkali olivine basalt; 4,5=basanites (Table 1.4.2.1-37,36); 6,7=Karoo picrite (Table 1.4.2.1-13,16); 8=Servillleta basalt (Table 1.2.4.1-1); 9,10=lower and upper average Deccan traps (Table 1.2.3.6); 11=average Siberian trap (Table 1.2.2.13a-219); 12=Keweenawan diabase (Table 1.2.2.19-6); 13=Baffin Island olivine tholeiite (Table 1.2.6.14); 14=Barberton Mt. Komatiite (Table 1.4.2.1-3).

low-SiO_2 liquids than in high-SiO_2 liquids (Ryerson and Hess, 1980). Consequently, even though granitic liquids might be saturated in Ti-rich and P-rich phases, the concentrations will be quite low as indicated by the granitoid points. However, the solubility of K is high in both high-and low-SiO_2 liquids, so its concentration may be high or low over a wide range of silica. Al_2O_3 concentration serves as an index of plagioclase saturation. Superimposed on the igneous compositions in Fig. 1 is a set of four liquid lines of descent (LLD) calculated at 11 kbar with a version of MAGFOX (Longhi, 1991) modified for high pressures. Each LLD represents approximately fractional crystallization of 80% of the original. The set (Table 1) includes an ocean island basalt (H_0) that is the more aluminous of the two parent magmas calculated for Kilauea by BVSP (1981); an olivine tholeiite (BI_0) that is from Baffin Island and reportedly (Clarke, 1970) has strong MORB affinities; a picrite (K_0) that is from the Karoo flood basalt

Table 1
Bulk compositions modeled (wt.% oxides)

	Baffin Is. Tholeiite	Kilauea Parent	Bezi Dike (Karoo)	Barbeton Komatiite	Post-Archean mafic crust	Fe-PUM	HK66
Reference	BVSP (1981) Table 1.2.3.7	BVSP (1981) Table 1.2.6.14	BVSP (1981) Table 1.4.2.1	BVSP (1981) Table 1-4-2-1	Rudnick and Fountain (1995)	After Hart and Zindler (1986)	Takahashi and Kushiro (1983)
SiO_2	48.38	49.14	49.80	45.97	51.14	46.10	48.02
TiO_2	0.99	1.38	2.88	0.20	1.30	0.18	0.22
Al_2O_3	14.06	11.26	9.21	3.87	16.49	4.07	4.88
Cr_2O_3	0.13	0.10	0.10	0.42	0.03	0.47	0.25
FeO	10.56	11.26	11.00	11.02	9.75	10.03	9.9
MgO	12.02	14.85	14.88	32.60	7.57	35.43	32.35
MnO	0.17	0.10	0.15	0.21	0.19	0.13	0.14
CaO	11.92	9.21	7.40	5.04	10.06	3.22	2.97
K_2O	0.10	0.410	1.98	0.19	0.64	0.03	0.07
Na_2O	1.56	2.05	2.08	0.48	2.60	0.07	0.66
P_2O_5	0.10	0.23	0.52	0.01	0.23	0.02	0.07
Mg′	0.670	0.701	0.607	0.841	0.581	0.864	0.857

province and has a highly fractionated incompatible element pattern (Hawkesworth et al., 1984); and a Barberton Mt. komatiites (B_0) that has relatively high K_2O (Green et al., 1975).

3.1. Fractional crystallization

Thick lines represent the calculated fractional crystallization paths in Fig. 1. The first appearance of plagioclase in the 4 LLDs is marked by the transition from shaded (plagioclase-undersaturated) to solid (plagioclase-saturated) lines. Several compositional features in Fig. 1 are relevant to the petrogenesis of massif anorthosites. First, there is an apparent trend among the anorthosite parental magmas (squares) of increasing TiO_2, K_2O, and P_2O_5 with decreasing Mg′. The trend appears to consist of two separable groups: one with lower concentrations of the three incompatible elements and higher Mg′; the other with high concentrations of incompatible elements and lower Mg′. These two groups correspond roughly to "labradorite" and "andesine" types of anorthosites (Anderson and Morin, 1968). The overall trend is steeper than any of the calculated fractionation paths, suggesting that simple fractionation of any of the basaltic magmas cannot account for the range of compositions. If one argues that the lower Mg′ values of the andesine anorthosites are indications that the andesine anorthosites are relatively more evolved than their labradoritic counterparts, then the calculations suggest that back fractionating the andesine anorthosites would produce compositions with higher Mg′, but relatively similar TiO_2, K_2O, and P_2O_5. The overall effect would be to steepen the distribution of squares in Fig. 1, thus making fractional crystallization an even less suitable explanation of variation within the group of anorthosite parent magmas. Second, the Harp Lake data show that a single large complex may contain nearly all the variation found in the entire suite. Third, although differentiates of the array of mantle-derived magmas cover the entire range of TiO_2, K_2O, and P_2O_5 concentrations, none of the differentiates reaches plagioclase saturation in the range of Mg′ (0.5 to 0.6) appropriate to the more primitive anorthosite parent magmas. Not surprisingly, the two compositions with the highest Al_2O_3 concentrations (H_0 and BI_0) reach plagioclase saturation at the highest values of Mg′ (0.45).

3.2. Fractional crystallization with crustal assimilation

Several authors (Duchesne, 1984; Emslie, 1985; Morse, 1982) have previously observed that although the magmas from which massif anorthosites crystallized were basaltic in character, they were nonetheless compositionally distinct from other known basalts. Three general models thus emerge: in the first, the

anorthosite parent magmas start out as conventional basaltic magmas, but acquire their distinct compositions via melting and assimilation while ponded at the base of the crust (e.g., Ashwal, 1993); in the second, the anorthosite parent magmas derive their distinct compositions from melting a mafic source, (e. g., Duchesne, 1989; Duchesne and Demaiffe, 1978; Longhi et al., 1999; Taylor et al., 1984), which may be continental crust either heated from below or downthrust into the mantle (Duchesne et al., 1999) or it may be an overdense layered intrusion sinking back into the mantle (Glazner, 1994); in the third, the anorthosite parent magmas derive their distinct compositions from melting a distinct Fe-rich mantle mafic source (Olsen and Morse, 1990).

Proponents of the first model have concluded that the unique chemical signature of anorthosites derives from a mafic assimilant (Emslie et al., 1994)—clearly from Fig. 1, a granitoid assimilant would not be helpful in attaining or maintaining TiO_2, P_2O_5, or Al_2O_3 abundances. Accordingly, a second set of calculations was run to test the utility of a mafic assimilant. The material chosen was a 10-kbar partial melt of the TJ composition (TJ-7, Table 3 (Vander Auwera and Longhi, 1994)). The melt was saturated in plagioclase, orthopyroxene, and ilmenite, and possessed relatively high K_2O and P_2O_5 concentrations. The assimilant was added to the fractionating magma in increments proportional to the amount of crystallization: either 1 unit of assimilant per unit of

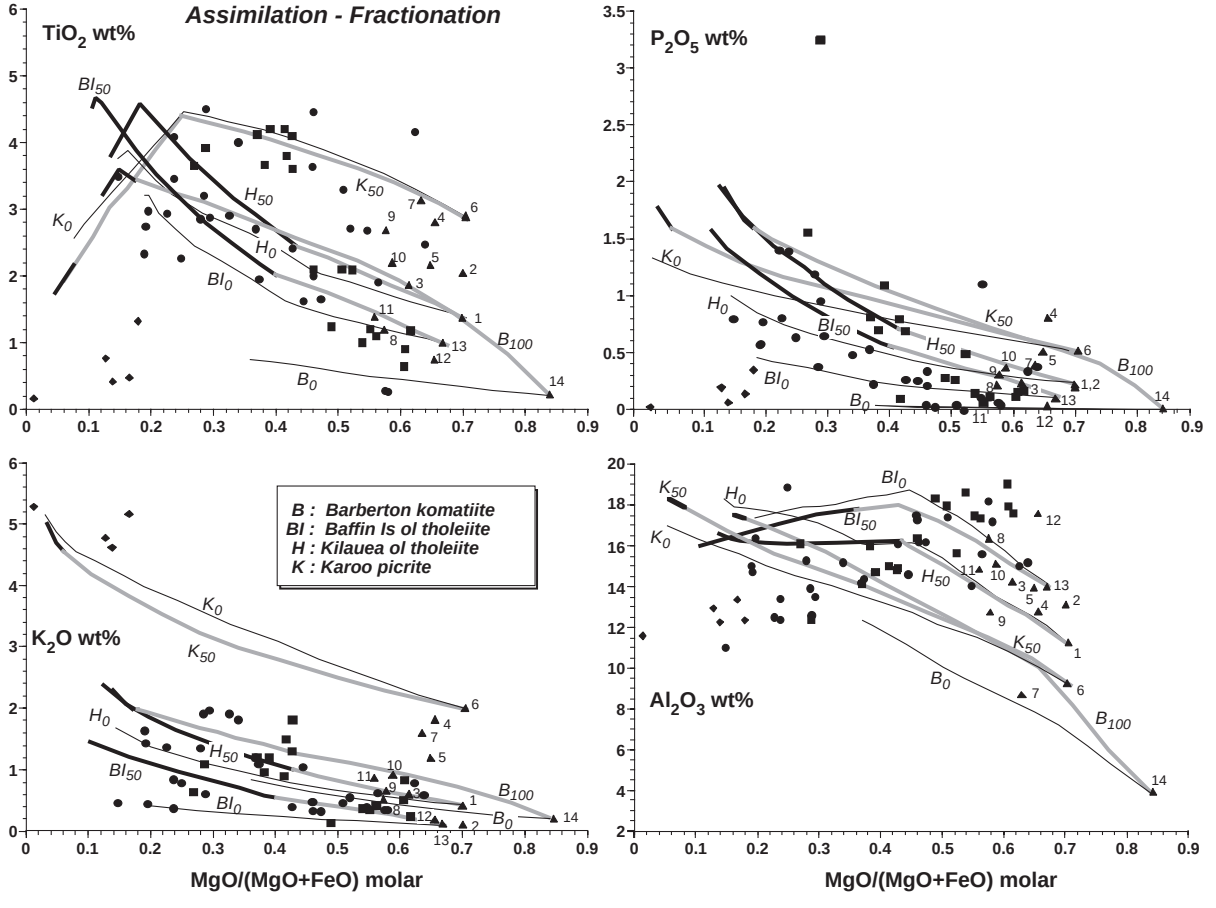

Fig. 2. Calculated assimilation fractional crystallization (AFC) paths of primitive basaltic magmas. Assimilation rate is either 50% or 100% as indicated by subscripts. Thin curves are fractional crystallization paths from Fig. 1. Symbols as in Fig. 1 except for parent magma compositions which are small squares here.

crystallization or 1 unit of assimilant per 2 units of crystallization. These assimilation rates yield 50% and 33% total assimilation, respectively. Assimilation was stopped when the calculated temperature of the fractionating liquid dropped to that of the assimilant, 1130 °C. Results are shown in Fig. 2 and Table 2. Uncontaminated LLDs from Fig. 1 are shown as the thinner lines; subscripted numbers indicate the percent assimilation per crystallization step; and as in Fig. 1, the shaded lines become solid only after plagioclase appears.

Assimilation coupled with fractional crystallization (AFC) may increase, decrease, or leave relatively unchanged the concentrations of an element in a LLD depending upon the concentration of the element relative to that in the original magma. The AFC process produced relatively modest changes in the LLDs of the three basaltic compositions at a 50% assimilation rate. Increasing the rate to 100% did not produce any significant changes relative to the uncontaminated LLDs, except for the komatiite composition. So only the komatiite LLD is shown at a 100% (1 for 1) assimilation rate. The BI and H magmas show the least response to assimilation because their higher Al_2O_3 concentrations give them the lower liquidus temperatures and thus lower assimilation potentials.

Table 2
Selected calculated phase compositions (wt.% oxides) of Baffin Island Tholeiite AFC LLD

Fractional crystallization/50 % assimilation rate				
Baffin Is. Tholeiite		Aug in, opx out	Plag in	Opx in
T, °C	1309	1268	1166	1107
Mol fraction crystallized	0	0.059[a]	0.458[b]	0.796
SiO_2	48.38	48.21	47.58	43.49
TiO_2	0.99	1.11	2.01	4.67
Al_2O_3	14.06	14.59	18.39	16.20
Cr_2O_3	0.13	0.12	0.02	0.01
FeO	10.56	10.76	13.44	20.97
MgO	12.02	10.67	5.03	1.56
MnO	0.17	0.17	0.20	0.29
CaO	11.92	12.31	9.39	6.38
K_2O	0.10	0.15	0.55	1.37
Na_2O	1.56	1.69	2.76	3.30
P_2O_5	0.10	0.14	0.53	1.51
Mg′—*liq*	0.670	0.639	0.400	0.117
Mg′—*ol*	0.861	–	–	–
Wo/En—*opx*		0.035/0.837	–	0.041/0.359
Wo/En—*aug*		0.305/0.592	0.364/0.458	0.387/0.236
An—*plag*			0.637	0.562

[a] First crystallization of augite.
[b] First crystallization of plagioclase.

The slopes of the AFC LLDs are still shallower than the trends of the anorthosite parent magmas in terms of TiO_2, K_2O, and P_2O_5 versus Mg′. As above, the Karoo picrite has sufficient TiO_2, K_2O, and P_2O_5 to account for these elements in nearly all massif anorthosites with the probable exception of P_2O_5 in Labrieville (Owens et al., 1993). Even at a 100% assimilation rate, the komatiite falls well short in TiO_2 and K_2O. Also, as above, none of the LLDs reaches plagioclase saturation at an appropriately high Mg′.

These compositional relations imply that fractional crystallization of a wide array of magma types coupled with assimilation of a mafic source can produce the range of minor element compositions observed in the anorthosite parent magmas, but there is no reason why such processes should also produce an organized trend—the effect should be a scattershot of compositions similar to that displayed by the primitive mantle-derived magmas, but with a wider range of Mg′. Combined with the relatively late appearance of plagioclase, these relations cast doubt on hypothesis that AFC processes involving familiar basaltic magmas and mafic assimilants produced magmas parental to massif anorthosites. However, there is more doubt to cast.

Another recognized feature of massif anorthosites is the generally low Wollastonite component of their plagioclase-saturated parental magmas, as evidenced (a) in the chill margins of associated mafic intrusions such as the Kiglapait (Nolan and Morse, 1986) and Bjerkrem–Sokndal (Robins et al., 1997) Complexes; and (b) by the prevalence of troctolitic–noritic and noritic mineral assemblages in anorthositic rocks (Longhi et al., 1999). To illustrate the effects of the AFC processes on the wollastonite component at plagioclase saturation, the results of the calculations shown above are next shown in terms of mineral components.

Fig. 3 shows the 4 LLDs from Figs. 1 and 2 projected from the Wollastonite, Orthoclase, and Ilmenite components. Fig. 4 shows the same LLDs projected from Plagioclase, Orthoclase, and Ilmenite. The phase boundaries are from Longhi et al. (1999).

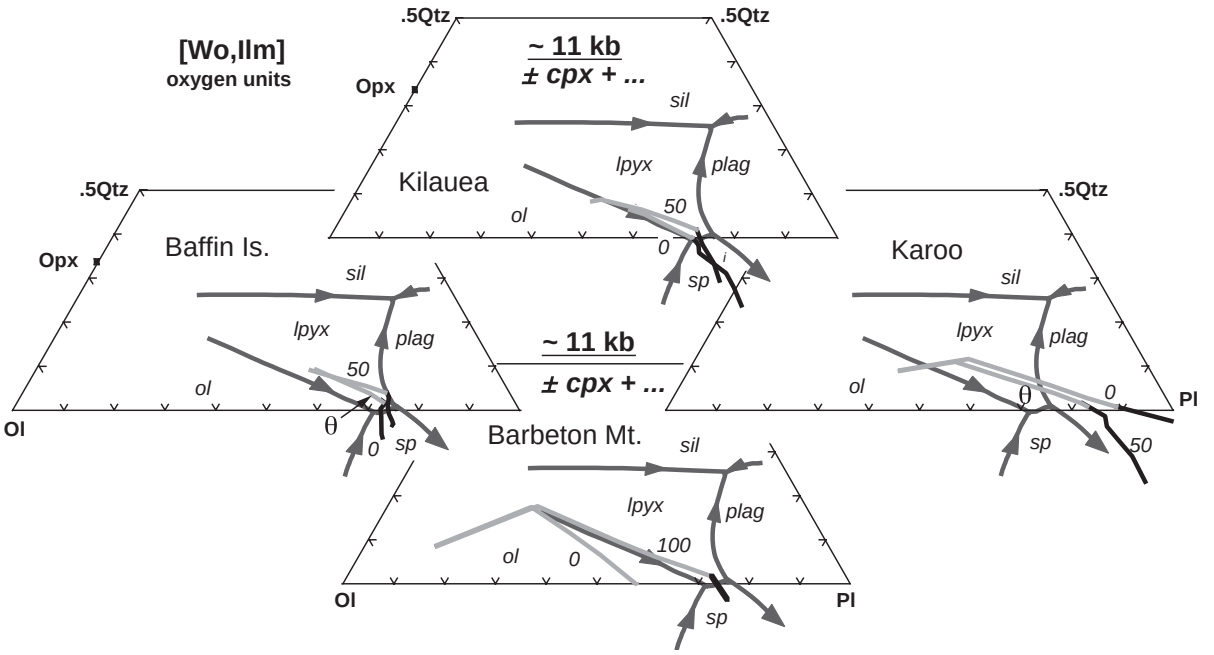

Fig. 3. Calculated fractional crystallization and AFC) paths from Fig. 2 projected from the Wo (Wollastonite), Or (Orthoclase), and Ilm (Ilmenite) components onto the Ol (Olivine)–Pl (Plagioclase)–Qtz (Quartz) component plane in terms of oxygen units after Longhi et al. (1999). Light shaded curves show 11.5-kb liquidus boundaries based on experimental data from Longhi et al. (1999). Arrows show direction of decreasing temperature. The symbol θ represents composition of HAOT from Bartels et al. (1991).

As above the shaded portions of the lines indicate a lack of plagioclase saturation. Generally, the curves record 80% fractional crystallization, and the crystallization sequence is olivine, then orthopyroxene, then augite, and then plagioclase. Olivine reacts out when orthopyroxene appears and orthopyroxene reacts out when augite appears. It should be obvious from Fig. 3 that most mantle-derived parental magmas require considerable crystallization to reach plagioclase saturation. It is also apparent that assimilation makes relatively little difference in the overall LLD. The reasons for the modest effects of assimilation are that the proportion of assimilant added in each step is small (<1%) relative to the body of fractionating liquid and that the mafic assimilant lies close to the traces of the LLDs (at least in some projections). Important exceptions occur when assimilant and the crystallizing phases are situated on opposite sides of a peritectic curve or the assimilant is far removed from the LLD. In such cases assimilation may either pull the LLD off the liquidus boundary or it may change the crystallization sequence. For example, Longhi et al. (1983) showed that assimilation of granite by komatiite could change the order of pyroxene appearance from olivine→augite to olivine→orthopyroxene. In the present case assimilation allows the LLD to reach plagioclase saturation after less crystallization of the komatiite and picrite magmas.

It is important to keep in mind that considerable portions of the LLDs are under-saturated with respect to plagioclase, so that in Fig. 4, the phase boundaries evidenced by abrupt changes in slope of the hollow portions of the LLDs are not shown and should be thought of as lying behind plagioclase saturation surface. Conversely, the onset of plagioclase crystallization has no effect on the trend of the LLD because plagioclase is a projection component. The most significant feature of Fig. 4 is that crystallization of most mantle-derived melts, with or without assimilation of a mafic source, drives the residual liquids to very high Wo components—the reason being a reaction relation between aluminous orthopyroxene and liquid to form aluminous augite. This relation

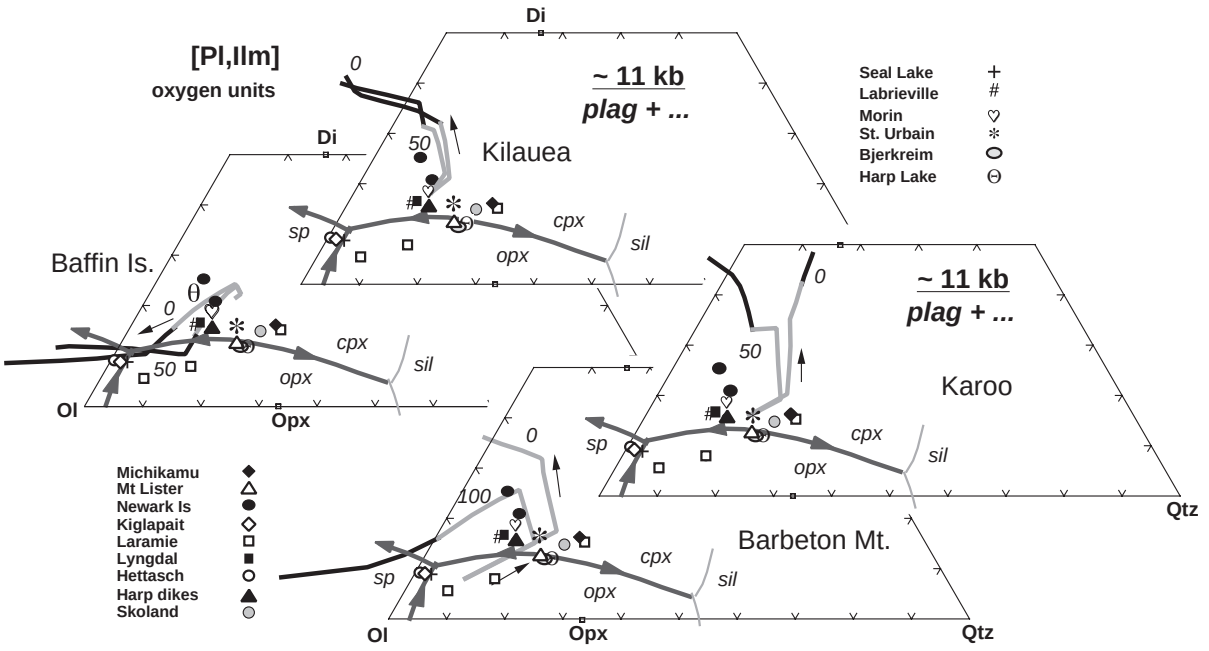

Fig. 4. Calculated fractional crystallization and AFC paths from Fig. 2 projected from the Pl, Or, and Ilm components onto the Ol–Qtz–Wo plane. Heavy shaded curves show 11.5-kb liquidus boundaries on the plagioclase-liquidus surface based on experimental data from Longhi et al. (1999). Squares from Figs. 1 and 2 (anorthosite parent magma compositions are now identified with individual symbols. References are given in Longhi et al. (1999).

itself is based on a tangent to the orthopyroxene/augite liquidus boundary in plagioclase undersaturated liquids intersecting the join of pyroxene compositions at a higher Wollastonite component than the coexisting augite. Thus all four mantle-derived melts arrive at the plagioclase saturation surface saturated with augite ± olivine; and three of the four are far removed from the locus of anorthosite parental magmas.

The LLD of the Baffin Island tholeiite, which has the highest Al_2O_3 concentration of the four modeled magma compositions (Fig. 1) and plots closest to the plagioclase saturation surface (Fig. 3), differs notably from the other three LLDs. It becomes saturated with orthopyroxene and augite after less than 6% crystallization, fractionates away from orthopyroxene saturation, and arrives at the plagioclase saturation surface after less than 50% crystallization. However, the liquid at this point, which is saturated only with augite and plagioclase, has a lower Wollastonite component than the combination of coexisting augite and plagioclase so that further crystallization of augite and plagioclase drives the liquid to even lower Wollastonite contents and eventually orthopyroxene re-precipitates, as evidenced by the abrupt change in slope of the LLD. Spinel does not crystallize in these liquids because their Mg′ values (0.11 at the end of the LLDs in Fig. 4) are too low: the orthopyroxene + augite + spinel + plagioclase (OASP) pseudo-invariant point projects near the trace of the Ol–Wo join at Mg′ = 0.45, but moves to lower silica compositions as Mg′ decreases (Longhi et al., 1999). Indeed, it must be remembered that Mg′ values of the BI_{50} residual liquids at plagioclase saturation are already too low for most of the anorthosite parent magmas, despite the appearance of the BI_{50} LLD sweeping across the traces of a number of the anorthosite parent magma compositions in Fig. 4.

These relations indicate that a subset of magmas with relatively high Al_2O_3 contents will fractionate close to the OASP pseudo-invariant point. If allowance is made for a higher Mg′ (perhaps inefficient fractionation), such magmas will have compositions within the range of some of the anorthosite parental magmas. However, as the LLDs for the Baffin Island tholeiite

demonstrate, a fractionating liquid will not dwell in this region of composition space nor move toward the cluster of anorthosite parental magma compositions that plot with higher Qtz component. Rather, the LLD trends away, as expected, from the array anorthosite parent magmas that lie close to pyroxene+plagioclase thermal divide. Crystallization of spinel would not stall the progress of this fractionation, but instead orthopyroxene would react out, and the liquid would evolve toward very-low SiO_2 compositions. The chemographic basis for this mode of crystallization is the projected arrangement of coexisting orthopyroxene+liquid at opposite corners of a quadrilateral formed by the tie lines between these phases and spinel+augite in Figs. 1 and 2 of Longhi et al. (1999). The equilibrium relation is thus opx+liq=sp+aug (+plag). Longhi et al. (1999) demonstrated that this particular relation develops between 7 and 10 kbar in response to liquidus boundaries shifting with pressure. Coupled with the observation that the trace of the pyroxene join becomes a thermal maximum at pressures ≥5 kbar (Longhi et al., 1999), the peritectic relation of orthopyroxene ensures that any liquid at the OASP point, whether differentiate or partial melt, will fractionate toward lower silica. Thus there is no possibility of generating the array of anorthosite parental magmas from liquids at the OASP point at pressures ≥7 kbar. Yet, such pressures are required for the formation of the orthopyroxene megacrysts (Longhi et al., 1993; Maquil and Duchesne, 1984).

The only way that assimilation can play a major role in anorthosite petrogenesis is if the major element characteristics of the anorthosite parent magmas are established at pressures <7 kbar. This condition implies that the HAOM are decoupled from the magmas that raft them upwards. Because the most aluminous of the HAOM form at 10 to 13 kb (Longhi et al., 1993; Maquil and Duchesne, 1984), this condition also leads to an implausible corollary that the major portion of assimilation occurs during ascent of plagioclase-rich suspensions, rather than in the ponded magma stage at greater depth where more heat and time are available.

3.3. Partial melting of mafic crust

In order to subject the partial melting of mafic crust hypothesis to the same scrutiny as the crystallization hypothesis, calculations of partial melting were carried out on a post-Archean mafic terrain (PAMT) composition from Rudnick and Fountain (1995) using a modified version of MAGPOX (Longhi, 2002). Partial results are listed in Table 3 and displayed in Figs. 5 and 6. The melt is saturated with orthopyroxene, augite, and plagioclase from the lowest calculated melt fraction (0.10) to the elimination of orthopyroxene at a melt fraction of 0.63. Fig. 5 illustrates the melting curve plotted with the massif rock compositions from Figs. 1 and 2. Also shown as numbered triangles are compilations of granulitic xenoliths from Emslie et al. (1994) and of estimates of lower crustal rock compositions (Rudnick and Fountain, 1995). The trend of the PAMT melting curve is steeper than any of the LLDs, but is similar to those of the suite of anorthosite parent magma compositions and of the array of Harp Lake compositions. The melting curve does not cover the full range of Mg′ observed in the rocks. A source with higher Mg′ or TiO_2 is needed to match the St. Urbain and Bjerkreim points. Fig. 6 shows the PAMT melting trend together with the anorthosite parental magma compositions projected

Table 3
Selected phase compositions (wt.% oxides) calculated for partial melting of average post-Archean mafic crust[a] at 11 kb

Partial melting; no assimilation				
Post-Archean mafic crust	Plag out	Opx out	Ilm out	
T, °C	1200	1189	1128	1112
Mol fraction melted	0.98	0.655	0.123	0.048
SiO_2	51.21	50.87	48.48	48.24
TiO_2	1.32	1.76	4.41	3.26
Al_2O_3	16.74	16.57	15.81	16.37
Cr_2O_3	0.03	0.02	0.02	0.01
FeO	9.69	12.11	14.79	12.85
MgO	7.12	6.31	3.00	2.33
MnO	0.19	0.23	0.29	0.26
CaO	10.08	7.97	5.69	5.32
K_2O	0.66	0.92	2.64	3.49
Na_2O	2.65	2.80	3.03	3.06
P_2O_5	0.23	0.35	1.85	2.30
Mg′—*liq*	0.567	0.473	0.265	0.244
Mg′—*ol*	–	–	–	–
Wo/En—*opx*	–	0.037/ 0.762	0.038/ 0.599	0.039/ 0.583
Wo/En—*aug*	0.363/ 0.522	0.355/ 0.496	0.372/ 0.387	0.385/ 0.367
An—*plag*	0.620	0.605	0.526	0.500

[a] Rudnick and Fountain (1995).

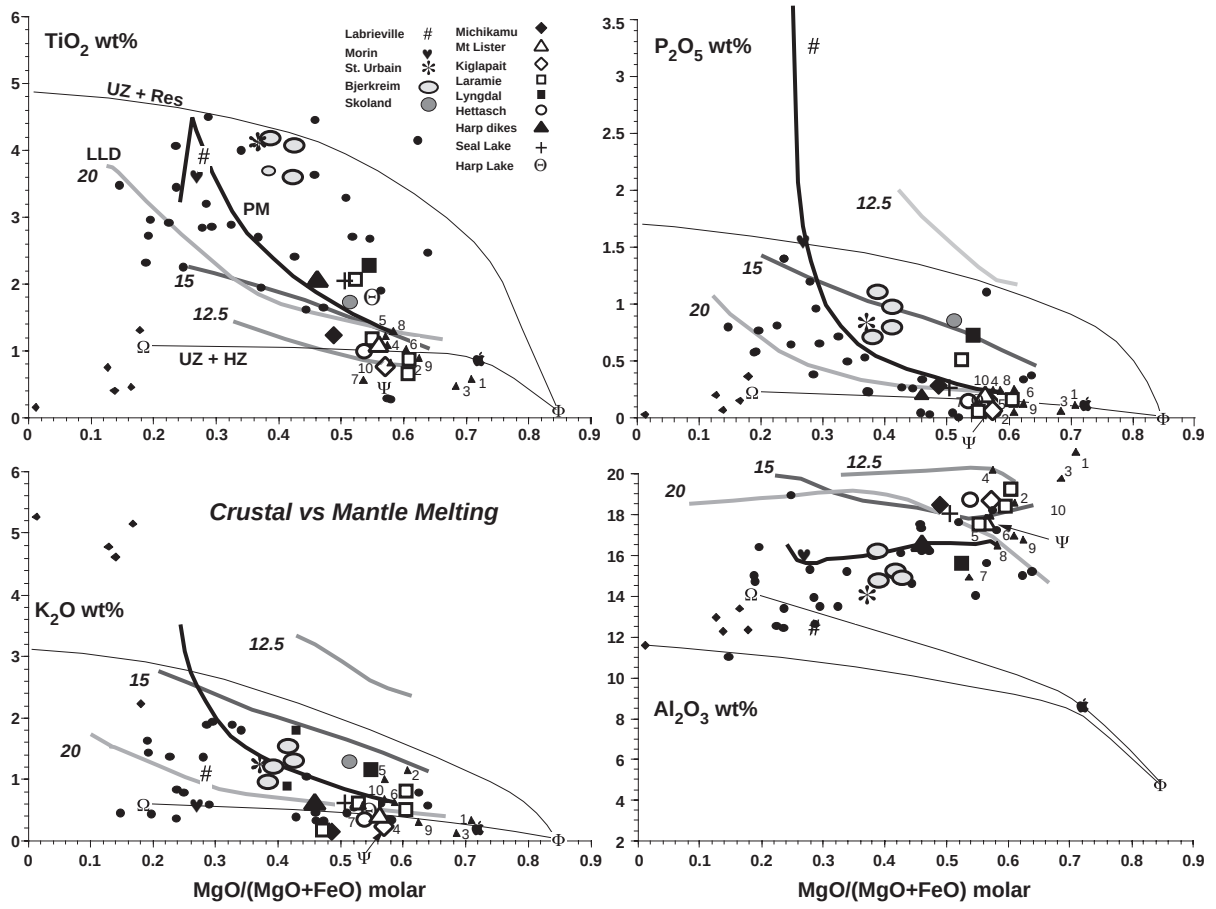

Fig. 5. Comparison of crustal and mantle melts. Solid dark curve = calculated equilibrium melting path at 11 kb for median post-Archean mafic terrain composition of Rudnick and Fountain (1995). Curves labeled with numbers are calculated 11-kbar LLDs of accumulated polybaric fractional melts. Numbers are pressures of initial melting. Melting stops after 12-kbar step. Details in text. Symbols as in Fig. 1. Numbered triangles are now xenoliths and mafic terrain compositions: 1–6—Arizona, New Mexico, Queensland, Massif Central, Mexico and grand average (Emslie et al., 1994); 7—median Archean mafic terrain, 8—median post-Archean mafic terrain, 9—median mafic xenoliths, and 10—median intermediate terrain (Rudnick and Fountain, 1995). Greek letters represent estimates of the Stillwater Ultramafic Zone (Φ), bulk (Ψ), and Hidden Zone (Ω) compositions (Hess, 1960); the represents a 50:50 mixture of the Φ and Ω compositions.

from the Plagioclase and Ilmenite components. Melting begins near the OASP point and then tracks the *opx + aug + plag* liquidus boundary curve to the point of orthopyroxene elimination in the residue. Thereafter the melting trend doglegs upward to reflect co-saturation in only augite and plagioclase until the composition is almost completely molten. Only a small increase in silica concentration would be needed for the locus of melts to be a virtual mirror image with onset of melting at or near the opx + cpx + sil + (plag) point and the upper part of the dogleg terminating near the Michikamu symbol. Although the calculated mafic melt compositions are much closer to the anorthosite parent magma compositions than are the calculated LLDs, Mg′ in this mafic melt is only 0.47 when orthopyroxene melts out and is only 0.57 at complete melting—still less than that of the most primitive anorthosite parent at 0.60. Thus mafic sources with higher Mg′ (~0.70) are required for at least some of the anorthosite parent magmas. Such compositions are readily available in the set of average crustal xenolith compositions from a number of localities tabulated by Emslie et al. (1994) that range in Mg′ from 0.57, similar to PAMT, to 0.72, as

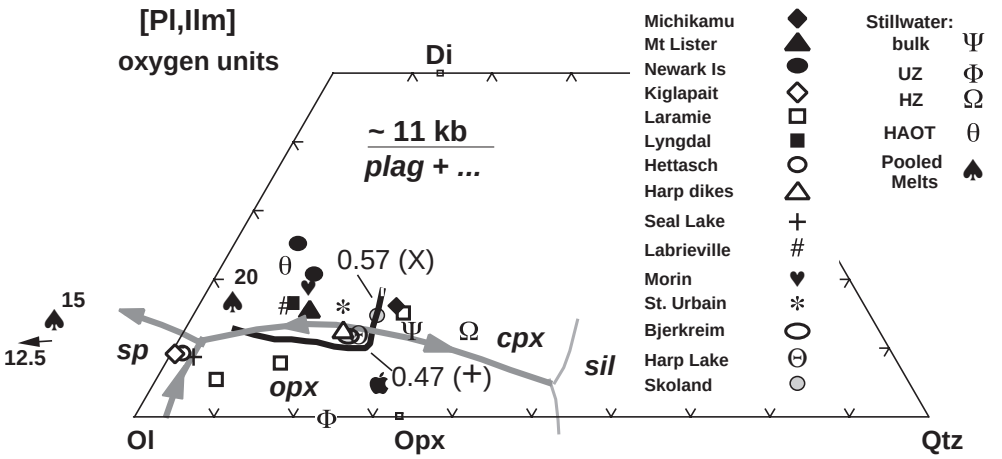

Fig. 6. Calculated equilibrium melting path at 11 kb for median post-Archean mafic terrain composition of Rudnick and Fountain (1995) plotted as in Fig. 4. Spades are accumulated polybaric melts (Table 4). Other symbols as in Fig. 5.

illustrated in Fig. 5. Partial melting of this array of compositions will generate liquids saturated with orthopyroxene, augite, and plagioclase that span the entire range of this liquidus curve from spinel to silica saturation. In particular, calculated partial melting of the average Queensland xenoliths (triangle 3 in Fig. 5) produces a melt saturated with plagioclase, orthopyroxene, and augite with Mg′=0.66. Nonetheless, the amount of melting required is >90% at a calculated temperature >1225 °C. So the crustal model requires an environment where high temperatures and extensive melting are possible.

In order to evaluate the suggestion that sunken layered intrusions might provide the mafic source for anorthosites, a few calculations were performed on relevant compositions. Estimates of the Stillwater Ultramafic zone (Φ), bulk (Ψ), and Hidden Zone (Ω) composition (Hess, 1960) are plotted in Figs. 5 and 6. The Stillwater bulk composition has Mg′ (0.57), which is too low to be a source for most anorthosite parent magmas; the concentrations of TiO_2, and P_2O_5 are also too low. The Ultramafic zone (UZ) has minor element concentrations that are too low (Fig. 5), plus a Wo content that is too low (Fig. 6); and the Hidden Zone (HZ) has Mg′ that is, of course, too low. The density distribution in layered intrusions offers a way around these shortcomings: the ultramafic zone of a noritic layered intrusion, like the Stillwater Complex, and the late stage cumulates are likely to be denser than the intermediate plagioclase cumulates. Therefore, an over-dense layered intrusion settling out of the crust might segregate mechanically with the ultramafic zone and late-stage cumulates sinking farther and faster than the intermediate cumulates. Mixtures of the ultramafic and late-stage cumulates provide an interesting range of source compositions. The incompatible partitioning of Ti, K and P ensures that such mixtures would have higher concentrations of these elements than the bulk composition at the same Mg′. Fig. 5 shows two sets of mixing curves: one between the Ultramafic and Hidden Zone compositions; the other between the Ultramafic zone and a liquid calculated with MAGFOX to represent 95% fractional crystallization at 3 kbar of Hess' (1960) bulk Stillwater estimate. The average Hidden Zone composition presumably includes intermediate and late-stage cumulates and thus is not truly representative of the late stage. The calculated residual liquid composition represents a plausible upper limit to the average composition of the late stage cumulates. So the area between the curves represents the range of mixtures of ultramafic and late-stage cumulates compositions. The minor element concentrations of most of the lower crustal compositions plot between the two mixing curves. An 11-kbar melting calculation of a 50/50 mixture of UZ and HZ components with bulk Mg′=0.72 (● in Fig. 5) produced a range of plagioclase-saturated melts that overlapped those in Figs. 5 and 6. However, because of the relatively low bulk Al_2O_3 evident in Fig. 5, plagioclase was

exhausted first and melting continued in the presence of orthopyroxene and augite. As was the case with the mafic terrain composition, the melt at the highest temperature where orthopyroxene, augite, and plagioclase coexisted had an Mg′ value (0.42) that was too low. Increasing the proportion of the late-stage component would have the effect of raising the mixing curves for TiO_2, K_2O, and P_2O_5 in Fig. 5 thereby making possible mafic melts with higher Mg′ and sufficient abundances of the minor elements. However, adding more of the late-stage component also reduces the bulk Al_2O_3, which reduces the melting range of plagioclase and the Mg′ of plagioclase-saturated melts, so not all mixtures of layered intrusions are likely to be appropriate source for massif anorthosites. Indeed, it is conceivable that foundered layered intrusions are the sources of only the group of parent magmas with higher Ti, K, and P, but lower Mg′. Although apparently no single source can melt to form the entire range of anorthosite parental magmas, the inherent variability in mafic terrains and layered intrusions makes generating these compositions feasible.

3.4. Direct melting

Direct production of a plagioclase-saturated magma by melting of peridotite is an important consideration at this point. Generating such melts is certainly possible in the laboratory at pressures ≤12 kb (Grove et al., 1992) and most MORB and high-alumina basalts (HAB) are plagioclase saturated, but closer examination of the question reveals some difficulties. First, the compositions of most sampled MORB are established only after crystallization of olivine and augite in the range of 2–8 kb (Grove et al., 1992; Langmuir et al., 1992). In other words, truly primitive MORB magmas are generally not plagioclase saturated. Modern hypotheses explain MORBs as blends of magmas generated over a range of pressure in small increments of decompression melting. Accumulated magmas, generated in this manner and then ponded near the base of the continental crust at pressures implied by the HAOM (10 to 13 kb), will have had little opportunity for melting in the plagioclase-peridotite stability field, and will thus be composed predominantly of increments with lower Al_2O_3 contents generated in the garnet- and spinel-peridotite fields. So a MORB-like petrogenetic environment dominated by pressure-release melting is unlikely to produce primitive plagioclase-saturated liquids. However, the presence of anhydrous high-Al olivine tholeiites (HAOT) in convergent plate margin environments (Grove et al., 2002) demonstrates that primary high-Al melts are possible under a different set of conditions. In any case, experiments on a primitve HAOT in the range of 10–15 kb have not revealed the presence of orthopyroxene (Bartels et al., 1991)—a necessary condition for anorthosite parent magmas. The projection point of the HAOT–the θ in Figs. 3 and 4–implies crystallization and AFC paths generally similar to the Baffin Island tholeiites (plagioclase and augite saturation relatively early, but orthopyroxene saturation late in a liquid that is fractionating away from the array of anorthosite parent magmas). These observations indicate that even though HAB magmas may reach plagioclase saturation at a sufficiently high Mg′, their Wo contents are still too high for the range of anorthosite parental magmas.

Of interest to students of anorthosite petrogenesis is the difference between the melting regimes of MORB and HAOT that allows depleted mantle to produce primitive plagioclase-saturated magmas in one case (HAOT), but not the other (MORB). It is generally accepted that mantle melts as it rises vertically beneath oceanic ridges and decompresses adiabatically. However, in the case of HAOT, current models of convergent margin magmatism show a horizontal component to decompression melting as mantle advects from the back-arc region to the volcanic front (Gaetani and Grove, 2003). Although there is surely some overlap, it appears that MORB petrogenesis typically involves decompression melting over a greater depth interval than the inclined melting of the HAOT source. There are several implications. First, more decompression means more melting, and melts produced at greater depths will be richer in FeO and MgO and poorer in Al_2O_3; conversely, melting over a shallower and more limited depth interval will produce a more aluminous blended magma. Second, less melt production means less depletion of incompatible elements, including Al_2O_3, in the residual mantle. Third, blends of melts produced over a shorter interval will be affected more

by melting at the top of the spinel-peridotite zone, where melts coexisting with peridotite may have Al_2O_3 concentrations in the range of 18–19 wt.% (Baker et al., 1995; Pickering-Whitter and Johnston, 2002). Decompression and cooling of such melts yield mixtures of plagioclase and liquid. These features qualitatively explain why primitive HAOT can be plagioclase saturated but not most MORB.

In order to explore the systematics of generating high-Al partial melts, several sets of polybaric fractional fusion calculations were carried on three model compositions: one was a variation of the primitive upper mantle composition of Hart and Zindler (1986) with lower Mg′ (Fe-PUM); a second was the depleted PUM (dPUM) composition of Kinzler and Grove (1992); and the third was a harzburgitic peridotite (HK66—Takahashi and Kushiro, 1983) with lower Mg′ (0.85) than typical mantle (0.89–0.90). The calculations were similar to those presented by Longhi (1992), but updated with newer algorithms for phase equilibria (Longhi, 2002 and 2003). Also, in the new calculations the amount of melting per unit of decompression is controlled by the heat of fusion of the source plus the heat equivalent of the temperature difference between the drop in temperature along the adiabat and the temperature drop along the solidus. Partial results are shown in Fig. 5 and listed in Table 4.

The 11-kbar liquid lines of descent for three accumulated polybaric melts of a Fe-PUM source are shown in Fig. 5 and listed in Table 4. In each case the calculation was stopped at after melting at 12 kbar. What distinguishes the three melts is the pressure of initial melting. In this case, pressures of 20, 15, and 12.5 kbar yield progressively lower temperatures, smaller melt fractions, and higher Al_2O_3 concentrations (Table 4). The 15- and 12.5-kbar pooled melts qualify as high-Al liquids, but not the 20-kbar liquid, which contains only 15 wt.% Al_2O_3. The 15- and 12.5-kbar pooled melts are plagioclase saturated; the 20-kbar liquid reaches plagioclase saturation after 30 % crystallization. As shown in Fig. 5, LLDs of the accumulated magmas have relatively shallow slopes, similar to those in Figs. 1 and 2. Therefore, in order to cover the range of incompatible element concentrations in the rocks, the primary magmas must have nearly the same range of concentrations. In Fig. 5, this is the case for K_2O and P_2O_5, which vary by a factor of 6, but not TiO_2. TiO_2 concentration in the accumulated melts actually decreases as the degree of melting decreases, remains nearly constant between the 20-kbar initial and the 15-kbar initial and then

Table 4
Calculated compositions (wt.% oxides) of accumulated polybaric melts of Fe-enriched primitive mantle

Mantle source	Fe-PUM[#]	Fe-PUM[#]	Fe-PUM[#]	dPUM	HK66	HK66
Pressure (kbar) of initial melting	20	15	12.5	12.5	15	12.5
T, °C (final)	1352	1271	1191	1226	1231	918
Wt fraction melted	0.079	0.024	0.0048	0.020	0.062	0.0080
SiO_2	48.34	51.66	56.08	52.74	54.75	63.47
TiO_2	1.18	1.04	0.79	1.00	0.96	0.39
Al_2O_3	14.78	18.71	19.92	18.37	16.80	19.28
Cr_2O_3	0.29	0.18	0.11	0.17	0.08	0.01
FeO	10.92	7.73	5.16	5.07	6.70	1.46
MgO	12.20	6.31	4.82	7.11	5.85	1.04
MnO	0.17	0.13	0.10	0.11	0.12	0.03
CaO	8.75	6.63	4.58	8.62	6.91	2.59
K_2O	0.40	1.17	2.40	0.68	1.10	4.60
Na_2O	2.98	4.97	6.03	5.76	6.73	7.11
P_2O_5	0.20	0.57	1.20	0.37	–	–
Mg′—*liq*	0.666	0.642	0.625	0.714	0.609	0.558

Calculations employ modified version of BATCH (Longhi, 2002); melting takes place in 0.5-kbar steps; the amount of melting in each step is balanced between the adiabatic gradient and the drop in temperature between steps; all melt above a residual porosity of 0.008 is removed from the source and accumulated; the last increment of melting takes place at 12 kbar in each case.

[#] Based on the primitive upper mantle composition of Hart and Zindler (1986).

decreases between the 15- and 12.5-kbar initials. Consequently, partial melting of Fe-PUM produces sufficient K_2O and P_2O_5 for anorthosite parentage, but not TiO_2.

The decrease of TiO_2 concentrations in the liquid at low-degrees of melting was first pointed out by Baker et al. (1995). Hirschmann et al. (1998) explained the effect as resulting from change in the Ti-partition coefficient between clinopyroxene and liquid from incompatible to neutral in response to increasing concentrations of alkalis with lower degrees of melting. Because alkalis reach their greatest potential enrichments at pressures (10–12 kbar) at the upper limit of the spinel-peridotite zone (Longhi, 2002), it becomes impossible to enrich a partial melt in TiO_2 at these pressures, even without the presence of an oxide phase. A calculation of 12.5 to 12.0 (12.5/12) kbar polybaric fractional melting of a depleted PUM source shows a higher TiO_2/K_2O ratio than the Fe-PUM analog (Table 4), TiO_2 remains far to low to produce the concentrations typical of the andesine anorthosites. The prospects for deriving anorthositic parent magmas from the harzburgitic peridotite, HK66, are even more remote. In this composition, the K_2O concentration in the 15/12 calculation is adequate for the labradoritic anorthosites, and K_2O concentration in the 12.5/12 calculation is more than sufficient for the andesitic anorthosites, but the TiO_2 produced in the 15/12 and the 12.5/12 calculations is too low for even the labradoritic anorthosites (Table 4). These considerations suggest that conventional pressure release melting of mantle peridotite is unlikely to produce a high-Al melt with high TiO_2 and K_2O concentrations typical of the more evolved, andesine anorthosites.

4. Implications

Calculations of 11 kbar LLDs with and without assimilation for several primitive mafic compositions, including komatiite, fail to match the compositions of magmas parental to the Proterozoic (massif) anorthosites. In all of the cases, differentiating magmas reach plagioclase saturation at Mg′ values much lower than those of magmas parental to the anorthosites. For a wide range of compositions, orthopyroxene reacts out with the appearance of augite well before the liquid reaches plagioclase saturation and, as a consequence, the derivative liquids upon reaching plagioclase saturation have Wo contents far higher than the anorthosite parent magmas and no possibility of re-saturation with orthopyroxene. Only the most aluminous of the four compositions modeled reached simultaneous saturation with plagioclase and orthopyroxene, but only in the late stages when Mg′ was too low. These relations suggest that a similar composition undergoing less efficient fractional crystallization would satisfy the Mg′ constraint as well as those of orthopyroxene and plagioclase saturation. However, as the efficiency of fractional crystallization decreases, the process quickly becomes indistinguishable from partial melting of a mafic source.

Partial melting of mafic sources is not without its problems, however. Although partial melting of sources ranging in composition from average post-Archean mafic crust (Rudnick and Fountain, 1995) to lower crustal xenoliths (Emslie et al., 1994) produces melts that satisfy the Ti–K–P systematics of most Proterozoic anorthosites, very extensive (>75%) melting is required in some cases to produce the anorthosite parents with the highest Mg′ values. Melting of foundered layered intrusions requires lower degrees of melting, but also requires density segregation to enrich the source in high-Mg′ ultramafic cumulates plus Ti-rich and K-rich late-stage cumulates. Addition of an ultramafic component also drives down the Al_2O_3 concentration, which in turn causes plagioclase to melt out at a lower melt fraction, thus making it more difficult to obtain sufficiently high (≥ 0.62) Mg′ values. Some of the conceptual difficulties of high degrees of melting are alleviated by appealing to deep thrusts of crust into the mantle (Duchesne et al., 1999) where ambient temperatures approaching the peridotite solidus (1272° at 12 kbar, Hirschmann, 2000) are higher than liquidus temperatures of many mafic compositions.

Alternatively, partial melting of anomalously ferroan peridotite might produce high-Al melts saturated with olivine, orthopyroxene, augite, plagioclase, and spinel, as has been observed in experiments on synthetic compositions (Grove et al., 1992; Scoates, 2003). But the peridotite would also need to be unusually high in TiO_2 because in the uppermost mantle, Ti changes from an incompatible to neutral element in response to the high alkali concentrations

that develop at the low degrees of melting needed to produce a high-Al melt enriched in K. Also, the combination of lower degrees of melting and higher concentrations of alkalis produces nepheline-normative pooled melts that become progressively undersaturated with smaller extents of melting as shown by the projection points of the three pooled melts in Fig. 6. Furthermore, even with a set of peridotites designed specifically to meet the Ti–K–P requirements of the suite of anorthosite parent magmas, the melt compositions would plot close to the OASP point in Fig. 6, but would be incapable of generating the anorthosite parent magma compositions which lie close to the pyroxene+plagioclase thermal divide. The orthopyroxene peritectic relation in liquids saturated with orthopyroxene+augite+plagioclase+spinel or with orthopyroxene+augite+plagioclase+olivine (Longhi et al., 1999) guarantees that such liquids will fractionate away from the thermal divide and the bulk of the parental compositions. Thus the weight of evidence favors melting mafic sources as the best way to produce magmas parental to the Proterozoic anorthosites at 10 to 13 kbar that straddle both the high- and low-silica sides of the plagioclase+pyroxene thermal divide.

Acknowledgements

This paper would not have been possible without the imagination, guidance, and generosity of Jean-Clair Duchesne. This paper also benefited from thoughtful, critical comments by Tony Morse and an anonymous reviewer.

The research was supported by NASA grants NAG-9-329 and NAG5-12074. Lamont-Doherty Earth Observatory Contribution no. 6760.

References

Anderson Jr., A.T., Morin, M., 1968. Two types of massif anorthosites and their implications regarding the thermal history of the crust. In: Isachsen, Y.W. (Ed.), Origin of Anorthosites and Related Rocks. New York State Museum and Science Service Memoir, Albany, pp. 47–55.

Ashwal, L.D., 1993. Anorthosites. Springer-Verlag, Berlin. 422 pp.

Ashwal, L.D., Wooden, J.L., 1983. Isotopic evidence from the eastern Canadian Shield for geochemical discontinuity in the Proterozoic mantle. Nature 306, 679–680.

Baker, M.B., Hirschmann, M.M., Ghiorso, M.S., Stolper, E.M., 1995. Compositions of near-solidus peridotite melts from experiments and thermodynamic calculations. Nature 375, 308–311.

Bartels, K.S., Kinzler, R.J., Grove, T.L., 1991. High-pressure phase-relations of primitive high-alumina basalts from medicine lake volcano, Northern California. Contrib. Mineral. Pet. 108, 253–270.

Basaltic Volcanism Study Project, 1981. Basaltic Volcanism on the Terrestrial Planets. Pergamon, New York. 1286 pp.

Berg, J.H., 1977. Dry granulite mineral assemblages in the contact aureoles of the Nain Complex Labrador. Contrib. Mineral. Pet. 6, 32–52.

Clarke, D.B., 1970. Tertiary basalts from Baffin Bay: possible primary magma from the mantle. Contrib. Mineral. Pet. 25, 203–224.

Duchesne, J.C., 1984. Massif anorthosites: another partisan review. In: Brown, W.L. (Ed.), Feldspars and Feldspathoids. Reidel, Boston, pp. 411–433.

Duchesne, J.C., 1989. Origin and evolution of monzonorites related to anorthosites. Schweiz. Mineral. Petrogr. Mitt. 70, 189–198.

Duchesne, J.C., Demaiffe, D., 1978. Trace elements and anorthosite genesis. Earth Planet. Sci. Lett. 38 (1), 249–272.

Duchesne, J.C., Hertogen, J., 1988. Le magma parental du lopolithe de Bjerkreim–Sokndal, Norvège méridionale. Comptes Rendus de l'Acadamie des Sciences Paris 306, 45–48.

Duchesne, J.C., Wilmart, E., 1997. Igneous charnockites and related rocks from the Bjerkreim–Sokndal layered intrusion (Southwest Norway). A jotunite (Hypersthene monzodiorite)-derived A-type granitoid suite. J. Pet. 38, 337–369.

Duchesne, J.C., Liegeois, J.P., Vander Auwera, J., Longhi, J., 1999. The crustal tongue melting model and the origin of massive anorthosites. Terra Nova 11 (2–3), 100–105.

Emslie, R.F., 1980. Geology and petrology of the Harp Lake Complex, central Labrador: an example of Elsonian magmatism. Geol. Surv. Can. Bull. 293, 1–136.

Emslie, R.F., 1985. Proterozoic anorthosite massifs. In: Tobi, A.C., Touret, J.L.R. (Eds.), The Deep Proterozoic Crust in the North Atlantic Provinces. Dordrecht, Netherlands, pp. 39–60.

Emslie, R.F., 1991. Granitoids of rapakivi granite–anorthosite and related associations. Precambrian Res. 51 (1–4), 173–192.

Emslie, R.F., Hamilton, M.A., Theriault, R.J., 1994. Petrogenesis of a Midproterozoic anorthosite–mangerite–charnockite–granite (AMCG) complex—isotopic and chemical evidence from the Nain Plutonic Suite. J. Geol. 102 (5), 539–558.

Fram, M., Longhi, J., 1992. Phase equilibria of dikes associated with Proterozoic anorthosite complexes. amer. Mining 77, 605–616.

Gaetani, G.A., Grove, T.L., 2003. Experimental constraints on melt generation in the mantle wedge, in Inside the Subduction Factory. Geophysical Monograph, vol. 138. American Geophysical Union, pp. 107–134.

Glazner, A.F., 1994. Foundering of mafic plutons and density stratification of continental crust. Geology 22, 435–438.

Green, D.H., Nichols, I.A., Viljoen, M., R., V., 1975. Experimental demonstration of the existence of peridotitic liquids in the earliest Archean. Geology 3, 11–14.

Grove, T.L., Kinzler, R.J., Bryan, W.B., 1992. Fractionation of mid-ocean ridge basalt (MORB), mantle flow and melt generation at mid-ocean ridges. Geophysical Monograph, vol. 71. American Geophysical Union, pp. 281–310.

Grove, T.L., Parman, S.W., Bowring, S.A., Price, R.C., Baker, M.B., 2002. The role of an H_2O-rich fluid component in the generation of primitive basaltic andesites and andesites from the Mt. Shasta region, N California. Contrib. Mineral. Pet. 142 (4), 375–396.

Hart, S.R., Zindler, A., 1986. In search of a bulk-earth composition. Chem. Geol. 57, 247–267.

Hawkesworth, C.J., Marsh, J.S., Duncan, A.R., Erlank, A.J., Norry, M.J., 1984. The role of continental lithosphere in the generation of the Karoo volcanic rocks; evidence from combined Nd- and Sr-isotope studies, Petrogenesis of the volcanic rocks of the Karoo Province. Special Publication—Geological Society of South Africa. Geological Society of South Africa, Johannesburg, pp. 341–354.

Hess, H.H., 1960. Stillwater igneous complex, Montana—a quantitative mineralogical study. Geol. Soc. Am. Mem. 80, 230.

Hirschmann, M.M., 2000. Mantle solidus: experimental constraints and the effect of peridotite composition. Geochem. Geophys. Geosyst. 1 (2000GC000070).

Hirschmann, M.M., Baker, M.B., Stolper, E.M., 1998. The effect of alkalis on the silica content of mantle-derived melts. Geochim. Cosmochim. Acta 62, 883–902.

Kinzler, R., Grove, T., 1992. Primary magmas of mid-ocean ridge basalts: 1. Experiments and methods. J. Geophys. Res. 97 (B5), 6885–6906.

Jansen, J.B.H., Blok, R.J.P., Bos, A., Scheelings, M., 1985. Geothermometry and geobarometry in Rogaland and preliminary results from the Bamble area. In: Touret, J.L.R. (Ed.), The Deep Proterozoic Crust in the North Atlantic Provinces. Dordrecht, Netherlands, pp. 499–516.

Langmuir, C.H., Klein, E.M., Plank, T., 1992. Petrological systematics of mid-ocean ridge basalts: constraints on melt generation beneath ocean ridges, Mantle Flow and Melt Generation at Mid-Ocean Ridges. Geophysical Monograph, vol. 71. American Geophysical Union, pp. 183–280.

Longhi, J., 1991. Comparative liquidus equilibria of hypersthene-normative basalts at low pressure. Am. Mineral. 76, 785–800.

Longhi, J., 1992. Origin of picritic green glass magmas by polybaric fractional fusion. Proc. Lunar Planet. Sci. Conf. 22, 343–353.

Longhi, J., 2002. Some phase equilibrium systematics of lherzolite melting. Geochem., Geophys., Geosyst. 3.

Longhi, J., 2003. A new view of lunar ferroan anorthosites: post magma ocean petrogenesis. J. Geophys. Res. 108.

Longhi, J., Wooden, J., Coppinger, K.D., 1983. The petrology of high-Mg dikes from the Beartooth Mountains, Montana: a search for the parent magma of the Stillwater Complex. J. Geophys. Res. 88, B53–B69 (Suppl.).

Longhi, J., Fram, M.S., Vander Auwera, J., Monteith, J., 1993. Pressure effects, kinetics and rheology of anorthositic and related magmas. Am. Mineral. 77, 605–616.

Longhi, J., Vander Auwera, J., Fram, M.S., Duchesne, J.C., 1999. Some phase equilibrium constraints on the origin of Proterozoic (massif) anorthosites and related rocks. J. Pet. 40 (2), 339–362.

Maquil, R., Duchesne, J.C., 1984. Géothermométrie par les pyroxènes et mise en place du massif anorthositique d'Egersund-Ogna (Rogaland, Norvège méridionale). Ann. Soc. Géol. Belg. 107, 27–49.

Morse, S.A., 1982. A partisan review of proterozoic anorthosites. Am. Mineral. 67 (11-1), 1087–1100.

Nolan, K.M., Morse, S.A., 1986. Marginal rocks resembling the estimated bulk composition of the Kiglapait Intrusion. Geochim. Cosmochim. Acta 50, 2381–2386.

Olsen, K.E., Morse, S.A., 1990. Regional Al–Fe mafic magmas associated with anorthosite-bearing terranes. Nature 344, 760–762.

Owens, B.E., Rockow, M.W., Dymek, R.F., 1993. Jotunites from the Grenville Province, Quebec: petrological characteristics and implications for massif anorthosite petrogenesis. Lithos 30, 57–80.

Pickering-Witter, J., Johnston, A.D., 2000. The effects of variable bulk composition on the melting systematics of fertile peridotitic assemblages. Contrib. Mineral. Pet. 140, 190–211.

Robins, B., Tumyr, O., Tysseland, M., Garman, L.D., 1997. The Bjerkreim–Sokndal layered intrusion, Rogaland, SW Norway: evidence from marginal rocks for a jotunite parent magma. Lithos 39, 121–133.

Rudnick, R.L., Fountain, D.M., 1995. Nature and composition of the continental crust: a lower crustal perspective. Rev. Geophys. 33, 267–309.

Ryerson, F.J., Hess, P.C., 1980. The role of P_2O_5 in silicate melts. Geochim. Cosmochim. Acta 44, 611–624.

Scoates, J.S., 2003. Constraining the source of Proterozoic anorthosites. Geol. Soc. Am. Bull. Abstracts (Annual Meeting), pp. 161–166.

Scoates, J.S., Frost, C.D., 1996. A strontium and neodymium isotopic investigation of the Laramie anorthosites, Wyoming, USA: implications for magma chamber processes and the evolution of magma conduits in Proterozoic anorthosites. Geochim. Cosmochim. Acta 60 (1), 95–107.

Takahashi, E., Kushiro, I., 1983. Melting of a dry peridotite at pressures and basalt magma genesis. Am. Mineral. 68, 859–879.

Taylor, S.R., Campbell, I.H., McCulloch, M.T., McLennan, S.M., 1984. A lower crustal origin for massif-type anorthosites. Nature 311, 372–374.

Vander Auwera, J., Longhi, J., 1994. Experimental study of a jotunite: constraints on the parent magma composition and crystallization conditions, P, T, fO_2. of the Bjerkreim–Sokndal layered intrusion, Norway. Contrib. Mineral. Pet. 118, 60–78.